



This is a repository copy of *Edge orientation signals in tactile afferents of macaques*.

White Rose Research Online URL for this paper:  
<http://eprints.whiterose.ac.uk/105343/>

Version: Accepted Version

---

**Article:**

Suresh, A.K., Saal, H.P. [orcid.org/0000-0002-7544-0196](https://orcid.org/0000-0002-7544-0196) and Bensmaia, S.J. (2016) Edge orientation signals in tactile afferents of macaques. *Journal of Neurophysiology*, 116 (6). pp. 2647-2655. ISSN 0022-3077

<https://doi.org/10.1152/jn.00588.2016>

---

**Reuse**

Unless indicated otherwise, fulltext items are protected by copyright with all rights reserved. The copyright exception in section 29 of the Copyright, Designs and Patents Act 1988 allows the making of a single copy solely for the purpose of non-commercial research or private study within the limits of fair dealing. The publisher or other rights-holder may allow further reproduction and re-use of this version - refer to the White Rose Research Online record for this item. Where records identify the publisher as the copyright holder, users can verify any specific terms of use on the publisher's website.

**Takedown**

If you consider content in White Rose Research Online to be in breach of UK law, please notify us by emailing [eprints@whiterose.ac.uk](mailto:eprints@whiterose.ac.uk) including the URL of the record and the reason for the withdrawal request.



[eprints@whiterose.ac.uk](mailto:eprints@whiterose.ac.uk)  
<https://eprints.whiterose.ac.uk/>

## **EDGE ORIENTATION SIGNALS IN TACTILE AFFERENTS OF MACAQUES**

Aneesha K. Suresh<sup>1</sup>, Hannes P. Saal<sup>2</sup>, & Sliman J. Bensmaia<sup>1,2</sup>

<sup>1</sup>Committee on Computational Neuroscience, University of Chicago, Chicago, IL

<sup>2</sup>Department of Organismal Biology and Anatomy, University of Chicago, Chicago, IL

## **ACKNOWLEDGMENTS**

We would like to thank Benoit Delhayé for helpful comments on a previous version of this manuscript. This work was supported by NSF grant IOS 1150209 and by NIH grant NS096952 (F31).

## **ABSTRACT**

The orientation of edges indented into the skin has been shown to be encoded in the responses of neurons in primary somatosensory cortex in a manner that draws remarkable analogies to their counterparts in primary visual cortex. According to the classical view, orientation tuning arises from the integration of untuned input from thalamic neurons with aligned but spatially displaced receptive fields (RFs). In a recent microneurography study with human subjects, the precise temporal structure of the responses of individual mechanoreceptive afferents to scanned edges was found to carry information about their orientation. This putative mechanism could in principle contribute to or complement the classical rate-based code for orientation.

In the present study, we further examine orientation information carried by mechanoreceptive afferents of Rhesus monkeys. To this end, we record the activity evoked in cutaneous mechanoreceptive afferents when edges are indented into or scanned across the skin. First, we confirm that information about the edge orientation can be extracted from the temporal patterning in afferent responses of monkeys, as is the case in humans. Second, we find that the coarse temporal profile of the response can be predicted linearly from the layout of the RF. Finally, we show that orientation signals in tactile afferents are often highly dependent on stimulus features other than orientation, which complicates putative decoding strategies. We discuss the challenges associated with establishing a neural code at the somatosensory periphery, where afferents are exquisitely sensitive and nearly deterministic.

## **INTRODUCTION**

Our ability to dexterously grasp and manipulate objects relies critically on our sense of touch, without which we would struggle to perform even the most basic activities of daily living (Witney et al. 2004; Johansson and Flanagan 2009). To successfully grasp and manipulate an object requires that we acquire information about the object at the contact points (Augurelle et al. 2003), including information about the orientation of local edges (Jenmalm and Johansson 1997; Jenmalm et al. 2000). Neurons in primary somatosensory cortex (S1) exhibit strong tuning for edge orientation in their firing rates, a tuning that is not observed in responses of cutaneous mechanoreceptive afferents (Bensmaia et al. 2008a). The orientation tuning in S1 draws a powerful analogy to that found in primary visual cortex (Pack and Bensmaia 2015), which is thought to originate from the integration of weakly tuned input from thalamic neurons with spatially displaced receptive fields, as first proposed by Hubel and Wiesel (Hubel and Wiesel 1962; Priebe and Ferster 2012).

The classical model of orientation coding in vision may not tell the whole story about how tactile edges are encoded, however. In recent microneurography experiments with human subjects, temporal spiking patterns of cutaneous mechanoreceptive afferents were shown to carry information about edge orientation not in their rates but in their precise spiking patterns. Indeed, the temporal sequence of spikes evoked by scanned bars in two types of tactile fibers – slowly adapting type 1 (SA1) and rapidly adapting (RA) afferents – differed depending on the orientation of the bars (Pruszynski and Johansson 2014). Receptive fields (RFs) comprise multiple hotspots (Johansson 1978) so scanning edges across the RF at different orientations excite the fiber's hotspots in different sequences, culminating in different spiking patterns. In principle, then, these orientation signals could contribute to the tuning in S1 or serve to complement a rate-based representation of edge orientation (Scholl et al. 2013).

In the present study, we investigated the nature of these orientation signals at the tactile periphery. First, we determined whether monkey afferents convey information about edge orientation in their responses. Next, we assessed the degree to which responses could be predicted from RF topography, as is the case in the human nerves. Third, we gauged the extent to which edge orientation signals in tactile afferents are robust to changes in other stimulus parameters, for example scanning direction or

indentation depth. Finally, we discuss the implications of these results on tactile orientation processing and consider the challenges associated with establishing a neural code at the somatosensory periphery.

## **METHODS**

### **Neurophysiology**

All experimental protocols complied with the guidelines of The Johns Hopkins University Animal Care and Use Committee and the National Institutes of Health's Guide for the Care and Use of Laboratory Animals. We recorded single units from the median and ulnar nerves of anaesthetized macaque monkeys using standard methods (Mountcastle et al. 1967; Talbot et al. 1968) as previously described in detail (Bensmaia et al. 2008a). Briefly, the forearm and hand were fixed by a clamp, and the ulnar or median nerve was exposed in the upper or lower arm. Next, a skin flap pool was formed, and a small bundle of axons was separated from the nerve trunk and wrapped around a silver electrode.

An afferent was classified as SA1 if it had a small RF and produced a sustained firing response to a skin indentation, as RA if it had a small RF and responded only at the onset and offset of an indentation, and as Pacinian (PC) if it had a large, diffuse RF and was activated by air blown gently over the hand. The point of maximum sensitivity (hotspot) was located using a handheld probe and the stimulus was centered on the hotspot. We only recorded the responses of RA and SA1 afferents with RFs located on the distal fingerpad of digits 2 through 5 (PC fibers were not included for analysis as their RF properties are ill suited to encode the spatial properties of isolated spatial features).

### **Stimuli**

#### Stimulator

Stimuli were delivered using a dense array tactile stimulator consisting of 400 probes arrayed in a 20 by 20 grid spanning 1 cm x 1 cm (Killebrew et al. 2007) (Figure 1A). Each probe was driven along the axis perpendicular to the skin's surface by a dedicated motor, under independent computer control. The stimulator is the tactile equivalent of a video monitor, endowing the experimenter with the ability to activate each pin independently to create arbitrary spatiotemporal patterns over an area of 1 cm<sup>2</sup>. Scanned bars were generated by sequentially activating neighboring pins on the array.

#### Single probe indentations

This stimulation protocol was used to characterize the receptive field topography. On each trial, a probe was indented into the skin for 100 ms at an amplitude of 300  $\mu$ m with an inter-stimulus interval of 100 ms. Consecutively indented probes were not adjacent to reduce confounding effects of skin mechanics (Pawluk and Howe 1997; Pawluk et al. 1998). To reconstruct each afferent's RF, we computed the mean of five responses to each of the 400 pins. The point of maximum sensitivity was selected as the hotspot.

#### Scanned bars

This protocol most closely matched that used in the previous study investigating orientation signals in the nerve (Pruszynski and Johansson 2014). On each trial, a bar was scanned across the fingertip in one of 16 directions, ranging from 0 to 337.5° in 22.5° steps (Figure 2, 0° corresponds to rightward motion) and one of three indentation depths (100, 200, and 300  $\mu$ m). Each direction and amplitude pair was presented five times in pseudorandom order, yielding a total of 240 trials. The scanning speed was 40 mm/s, and the inter-stimulus interval was 200 ms.

#### Indented bars

We wished to extend the results from the original study by examining whether afferent responses to indented edges also conveyed information about their orientation. Indeed, to the extent that

orientation signals are dependent on the sequential activation of multiple spatially displaced receptors innervated by a given afferent, responses to indented bars will not carry orientation information. On each trial, a bar was indented into the skin at one of 8 orientations, ranging from 0 to 157° in 22.5° steps (with 0° degrees corresponding to the long axis of the finger). The indentation depth of the bar was always 500  $\mu\text{m}$ , and its duration 30 ms. The bar was either indented in the center of the RF (determined from the RF map derived from the single probe indentations), or it was displaced by 1 to 5 mm along the axis normal to the orientation of the bar (for a total of 11 different locations at each orientation, Figure 1C). Bars were each presented 10 times for each orientation and location pair for a total of 880 trials.

## **Data Analysis**

### Metric space analysis for orientation classification

To assess the degree to which information about orientation is carried in the spiking responses of individual afferents, we implemented a classification analysis. Specifically, we wished to determine whether we could classify stimuli that differed in orientation based on the responses they evoked in individual afferents. We used a nearest neighbor classifier, which gauges whether spike trains evoked by a class of stimuli (bars at a specific orientation in this case) are more similar to each other than to those evoked by other classes of stimuli (bars at different orientations). We used spike distance as a measure of dissimilarity between two spike trains (Victor and Purpura 1997), as we have previously done (Mackevicius et al. 2012; Weber et al. 2013). In brief, spike distance is the smallest possible cost of transforming one spike train into another: There is a cost (of 1) associated with adding and deleting spikes, and a cost per unit time,  $q$ , associated with moving spikes. A benefit of this analysis is that, by varying the parameter  $q$ , we can manipulate the contribution of precise spike timing to the distance computation and thus to the classification analysis. If  $q$  is 0, then the distance amounts to computing the difference in spike count. As  $q$  increases, it becomes less and less advantageous to move spikes around rather than to add and subtract them, and so small differences in the timing of individual spikes increasingly determines spike distance. We modified this analysis by computing the pairwise spike distance between temporally shifted spike trains (shifted by 1ms increments, up to 100ms) and using the minimum distance across all shifts to ensure that classification did not exploit differences in absolute response latency, which is largely determined by the precise location of the RF relative to the stimulus. Using spike distance with different values of  $q$  is analogous to taking the cross correlation between spike trains convolved with filters at different widths (Pruszynski and Johansson 2014) but the temporal precision is more clearly defined with spike distance than for filtered spike trains and we found classification performance to be consistently higher with the former than with the latter (data not shown).

### Prediction of firing rates based on receptive field topography

To determine whether RF topography could predict firing profiles in response to edge orientation stimuli, we implemented a simple linear model. We predicted each afferent's response to scanned bars by convolving the empirically derived RF map with the time-varying stimulus pattern to gauge the degree to which the afferent's firing rate is shaped by the linear superposition of the receptive field area and the stimulus pattern (Pruszynski and Johansson 2014). We interpolated the RF map and stimulus pattern to achieve a temporal resolution of 2.5 ms in our response predictions. Model performance was quantified by cross correlating predicted firing profiles and the mean instantaneous firing profiles for each scanning direction.

To assess the temporal resolution at which predicted responses matched observed responses, we measured the cross-correlation of predicted responses and observed responses after filtering the

responses in different frequency bands. We used a 6<sup>th</sup> order bandpass Butterworth filter across the following frequency ranges: 333-500 Hz (2-3ms); 125-200Hz (5-8 ms); 66-100 Hz (10-15ms); 33-50Hz (20-33ms); 10-20Hz (50-100ms). We then cross-correlated band-passed predicted responses with band-passed observed responses at the frequencies ranges specified above. This way, we could determine which frequency band, or temporal resolution, elicited the highest correlation. We also computed the cross-correlation of observed responses to repeated presentations of each stimulus at the different frequency bands to establish the repeatability of the response within each band. We then assessed how close the predictions were to the best possible performance, fixed by the repeatability of the response within each frequency band. Specifically, we calculated the ratio between the mean  $R^2$  value for predicted vs. observed and that for observed vs. observed within each frequency range.

## RESULTS

We recorded the responses of 22 afferents (12 SA1 and 10 RA) to scanned bars and of a subset of these to indented bars (18 total: 10 SA1 and 8 RA, Figure 2).

### Edge orientation signals in afferent responses

Our first objective was to replicate the finding that the spiking responses of mechanoreceptive afferents carry information about the orientation of edges scanned across the skin in monkeys (Pruszynski and Johansson 2014). To this end, we attempted to classify the orientation of scanned edges based on the responses evoked in individual afferents. Specifically, we used a nearest neighbor classifier, which gauges the degree to which the responses to bars at a given orientation are similar to each other and different from those at different orientations. The dissimilarity between spike trains was measured using spike distance, which is the cost to transform one spike train into another (Victor and Purpura 1997). Adding or removing a spike incurs a cost of 1, moving a spike incurs a cost of  $q$  per millisecond. We performed the classification analysis at different values of  $q$  to determine the temporal resolution at which afferent signals are most informative about orientation.

#### *Scanned Bars*

Bars at 8 orientations (ranging from 0 to 167.5° in 22.5° steps) and three indentation levels (100, 200, and 300  $\mu\text{m}$ ) were scanned across each afferent's RF (see Figure 2). First, we classified orientation based on the spiking responses evoked in a single direction for each orientation (at an amplitude of 300  $\mu\text{m}$ ). That is, we split the data set in two, with each half containing afferent responses to each orientation in one of the two directions (each perpendicular to the bar's orientation). The classification analysis revealed that we orientation could be resolved with high fidelity (>90%) at a temporal resolution of ~2 ms (Figure 3A-C) with both SA1 and RA responses (averaged across both scanning directions), consistent with results obtained with human tactile afferents (Pruszynski and Johansson 2014). However, as temporal resolution decreased, discriminability markedly declined and was near chance at the coarsest temporal resolution, consistent with earlier observations that firing rates are not tuned for orientation (Bensmaia et al. 2008a). Furthermore, when we compared classification with the 300- $\mu\text{m}$  bars to that with shallower bars, we found that higher stimulus amplitudes resulted in better direction classification for SA1 fibers but not RA fibers, likely because the former exhibit higher response rates to higher amplitude stimuli but the latter do not (Figure 3D)(Blake et al. 1997). Finally, RA afferents were found to encode orientation substantially better than SA1 afferents, especially at lower indentation levels. Differences in performance may be attributable in part to the larger RF size of RA afferents (SA1:  $12.14 \pm 3.38 \text{ mm}^2$  SD; RA:  $24.32 \pm 7.35 \text{ mm}^2$  SD), which allows for a more temporally extended response to the same scanned stimulus and thus for more opportunity for the time-varying responses to differ across stimuli. Overall, these results demonstrate that individual afferent firing patterns convey information

about orientation in response to scanned bars (single direction) and do so in the precise timing of their spikes, replicating the result obtained with human tactile afferents (Pruszynski and Johansson 2014).

#### *Predicting responses from RF topography*

The orientation-specific spiking responses have been suggested to arise as a consequence of the sequential activation of spatially displaced receptors as the bar moves over each receptor in turn (Pruszynski and Johansson 2014). To test this hypothesis, we first investigated the degree to which a neuron's responses to scanned edges is shaped by the spatial arrangement of its transduction sites, replicating the model established in the human microneurography study (Pruszynski and Johansson 2014). To this end, we assessed the degree to which the spiking responses could be predicted from the linear superposition of RF topography and stimulus (Figure 4A-B). We found that the linear predictions matched the observed firing profiles, each in 1 ms bins, for both SA1 and RA afferents (Figure 4C) ( $r = 0.83 \pm 0.04$ , mean  $\pm$  s.d.), as was found with human afferents.

We then wished to determine the degree to which the predicted responses captured the fine temporal structure in their observed counterparts. To this end, we band-passed filtered the predicted and observed responses within multiple frequency ranges: 333-500 Hz (2-3ms); 125-200Hz (5-8 ms); 66-100 Hz (10-15ms); 33-50Hz (20-33ms); 10-20Hz (50-100ms). Next, we cross-correlated the filtered predicted and observed responses within each frequency band. We also cross correlated the filtered observed responses to repeated presentation of each stimulus amongst themselves to assess the degree to which responses were repeatable within each band. At the lower frequency ranges, and thus coarser temporal resolutions, the cross-correlations with the predictions became closer to the cross-correlations across repeats (Figure 4D). In other words, the coarse structure of the response is reflected in the linear prediction while its fine structure is not. Given that the orientation information is conveyed at a fine temporal resolution, it is likely that the spatial configuration of the RF is not sufficient to account for the orientation signals.

#### *Indented Bars*

To further test the sequential activation hypothesis, we investigated whether the spiking responses to indented bars carry orientation information even though the bar does not move relative to the RF. Each afferent was indented with bars at 8 different orientations, with the center of the bars positioned on the RF center or slightly shifted there from (by up to 5 mm in 1-mm steps in each direction, see Figure 1C). As was found with scanned bars, we achieved high classification performance at fine temporal resolutions ( $\sim 2$  ms) (Figure 3E), even when the indented bar was presented at an offset from the center of the RF of up to  $\sim 2$  mm in each direction (Figure 3F), as might be predicted from the measured RF size. This high level of classification performance is surprising given the short duration of the stimulus (30 ms).

In summary, then, individual afferents carry edge orientation information throughout their RF, even for indented bars, suggesting that the sequential contact with spatially displaced hotspots is not required for the genesis of precisely timed spiking patterns carrying orientation information.

#### *Testing the robustness of orientation signals across conditions*

A neural code for orientation would be robust to changes in other stimulus properties so that orientation information could be decoded by downstream structures regardless of the precise geometry of the edge or of its motion across the RF (or lack thereof). To the extent that orientation signals vary depending on other stimulus properties, decoding becomes more challenging and a biologically plausible theory of decoding must be formulated. For example, orientation signals dilate or contract systematically with decreases or increases in scanning speed (Pruszynski and Johansson 2014). In

principle, then, speed could in principle be corrected for when decoding orientation. Here, we wished to characterize whether the temporal spiking sequences that signal orientation depend on other stimulus properties, including their amplitude, movement direction, and precise location on the RF. To this end, we attempted to classify the orientation of stimuli that also differed in other stimulus parameters based on the evoked neuronal response. To the extent that the orientation signals were consistent across changes in other stimulus features, classification performance would be high.

First, we examined the effect of changes in indentation amplitude on classification performance. That is, we pooled responses to scanned bars at amplitudes of 100 and 300  $\mu\text{m}$ , and assessed whether responses at 200  $\mu\text{m}$  were more similar to their counterparts at 100 and 300  $\mu\text{m}$  when the orientation was the same than when it was different. We found that classification was poor under these circumstances (Figure 5A), despite the fact that classification performance was high at each amplitude separately (Figure 3D). That is, we could classify orientation when the amplitude was held constant, but not when it varied. These results suggest that orientation signals are amplitude-dependent.

Second, we gauged the degree to which information about the orientation of a scanned edge was consistent across scanning directions. To this end, we computed the distance between spike trains evoked in one direction to those evoked in the opposite direction and found that classification performance fell to chance levels (Figure 5A). That is, the spiking response to a given orientation scanned in a given direction is no more similar to the response to the same orientation scanned in the opposite direction than it is to the response to a different orientation. Orientation signals are thus highly dependent on scanning direction. To the extent that orientation signals are determined by the sequential activation of receptors, we might expect that the spiking pattern in one direction might match the reversed spike pattern in the opposite direction. We tested this hypothesis by comparing the responses to one direction with the reversed responses to the opposite direction (Figure 5B). Again, we found that classification was poor (Figure 5A), which constitutes further evidence that RF topography cannot completely account for the orientation information in afferent responses.

Third, we investigated the dependence of the orientation signals for indented bars on the precise location within the RF at which they were presented. To this end, we compared the responses evoked by bars offset by 1 mm from the RF center to those evoked by bars that were delivered at the RF center. We chose this range of offsets because our initial analysis revealed that orientation discriminability remained relatively constant over this range, when classification was performed at each location separately (Figure 3F). Again, we found that classification was poor, indicating that spiking patterns depend critically on the location of the stimulus within the RF (Figure 5C).

In conclusion, then, spike patterns evoked in the nerve depend not only on orientation but also on other stimulus features. In fact, the responses evoked by bars at the same orientation that differ in other ways are no more similar to each other than they are to responses to bars at different orientations. The strong susceptibility of afferent responses to influence from all stimulus features makes the decoding of orientation from these responses challenging.

## **DISCUSSION**

### *Explicit signaling of edge orientation by mechanoreceptive afferents*

We aimed to address the following three questions: 1) Do mechanoreceptive afferents of non-human primates carry edge orientation signals as do those of humans? 2) Can firing rate patterns be predicted from RF topography? 3) How robust are these edge orientation signals when other stimulus features vary?

First, our findings suggest that similar representations of edge orientation exist in human and non-human primates. Indeed, our analyses of data analogous to those from the previous human microneurography study (Pruszynski and Johansson 2014) – namely afferent responses to bars scanned in a single direction – yield results that are virtually identical. One minor difference between human and non-human afferents is that RA fibers seem to signal orientation better than do their SA1 counterparts, a discrepancy that can be attributed to differences in RF size. Indeed, some SA1 afferents have such tiny RFs that there is little opportunity for temporal modulation as the bar is scanned across the RF (see also Sripati et al. 2006). Such an effect might not be observed in humans because RA and SA1 receptive fields are more comparable to each other in size (Johansson 1978; Vallbo and Johansson 1984).

Second, we showed that, while the coarse temporal structure of afferent responses could be linearly predicted from the RF topography, the fine temporal structure could not. Since edge orientation signals rely on spiking patterns at the millisecond timescale, the fine spatial structure of afferent RFs topography is not sufficient to account for the resulting orientation information.

Finally, we explored the dependence of orientation signals on other stimulus features by testing the ability of classifiers to generalize across stimulus conditions. In the human microneurography study, afferent responses to scanned edges remained consistent across speeds, and were consistently warped in time depending on the speed (Pruszynski and Johansson 2014). Here, we aimed to explore the effect of other stimulus parameters, including those whose impact on cortical orientation signals and on human perception has been shown to be minimal (Bensmaia et al. 2008a, 2008b). We found that slight changes in the location at which the stimulus was delivered abolished the ability to classify its orientation, as did changes in amplitude or scanning direction. Given their dependence on other stimulus features, then, orientation signals can only be decoded in a context-dependent manner. In light of this, it is critical to articulate a biologically plausible decoder that could make use of these signals. Indeed, questions remain as to their role in perception or in motor control. Regarding the perceptual coding of orientation, one might ask whether these temporal orientation signals contribute to the robust rate-based orientation signals observed in S1, or complement them in some way. In motor control, information about the presence and orientation of edges would support the dexterous manipulation of objects. How such a susceptible signal might drive subtle adjustments of hand posture during object interactions has yet to be clearly articulated.

#### *Stimulus coding in tactile afferents*

Cutaneous mechanoreceptive afferents produce spiking responses that are (1) remarkably repeatable, with precision down to the sub-millisecond time scale (Johansson and Birznieks 2004; Mackevicius et al. 2012; Bale et al. 2015) and (2) exquisitely sensitive to skin stimulation. In other words, tactile fibers produce responses that are virtually identical when the same stimulus is presented repeatedly, and different when different stimuli are presented, even if these stimulus differences are very subtle. As a result, the information about stimulus identity in afferent responses is off the charts if spike timing is taken into consideration, particularly with good stimulus control that allows for precise repeated presentation of the same stimulus (Chagas et al. 2013). In other words, almost any pair of non-identical stimuli can be distinguished based on the spiking patterns they evoke in mechanoreceptive afferents. The key to understanding neural coding in the nerve, then, is to identify how different aspects of the afferent response systematically encode different aspects of the stimulus in such a way that these aspects can be decoded by downstream structures.

There are several ways to establish a neural code. One way is to demonstrate that information about a stimulus quantity, known to be accessible perceptually, is only carried in a given aspect of the neuronal response (Jacobs et al. 2009). For example, we have shown that the frequency composition of a skin vibration is encoded in the timing of the responses and that it cannot be decoded from their rates

(Mackevicius et al. 2012). Similarly, information about fine textures is only carried in the temporal spiking patterns evoked in RA and PC fibers (Weber et al. 2013). Another way is to demonstrate that an aspect of the neural response covaries with a stimulus property in the same way as does the corresponding perceptual dimension. For example, we have shown that, while several aspects of afferent responses change when the stimulus amplitude increases (firing rate, size of the activated population, etc.), one of these covaries more strongly than the others with the perceived magnitude of the stimulus (population firing rate weighted by afferent type), which strongly bolsters its claim as the neural code for intensity (Muniak et al. 2007). The third and probably most powerful way to confirm a neural code is to test it causally by artificially inducing a pattern of neuronal activation (through electrical or optogenetic stimulation, e.g.), and assessing whether it results in the predicted perceptual consequence. In a recent study, we confirmed the intensity coding hypothesis mentioned above by showing that it accounted for the perceived magnitude of electrically induced activation of the peripheral nerve (Graczyk, E.; Schiefer, M.; Delhay, B.; Saal, H.; Bensmaia, S.; Tyler 2016).

The remarkable sensitivity and precision of afferents presents a unique challenge in understanding how they encode stimulus information. There is little question that spike timing carries stimulus information and is behaviorally relevant (Saal and Bensmaia 2016). The orientation of edges impinging on the skin can theoretically be decoded from the temporal spiking patterns evoked tactile fibers. The challenge will be to determine how this is accomplished given the volatility of these signals.

## REFERENCES

- Augurelle A-S, Smith AM, Lejeune T, Thonnard J-L.** Importance of cutaneous feedback in maintaining a secure grip during manipulation of hand-held objects. *J Neurophysiol* 89: 665–671, 2003.
- Bale MR, Campagner D, Erskine A, Petersen RS.** Microsecond-Scale Timing Precision in Rodent Trigeminal Primary Afferents. *J Neurosci* 35: 5935–5940, 2015.
- Bensmaia SJ, Denchev P V, Dammann JF, Craig JC, Hsiao SS.** The representation of stimulus orientation in the early stages of somatosensory processing. *J Neurosci* 28: 776–786, 2008a.
- Bensmaia SJ, Hsiao SS, Denchev P V, Killebrew JH, Craig JC.** The tactile perception of stimulus orientation. *Somatosens Mot Res* 25: 49–59, 2008b.
- Blake DT, Hsiao SS, Johnson KO.** Neural coding mechanisms in tactile pattern recognition: the relative contributions of slowly and rapidly adapting mechanoreceptors to perceived roughness. *J Neurosci* 17: 7480–9, 1997.
- Chagas AM, Theis L, Sengupta B, Stüttgen MC, Bethge M, Schwarz C.** Functional analysis of ultra high information rates conveyed by rat vibrissal primary afferents. *Front Neural Circuits* 7: 1–17, 2013.
- Graczyk, E.; Schiefer, M.; Delhaye, B.; Saal, H.; Bensmaia, S.; Tyler D.** The Role of Sensory Adaptation in Artificial Tactile Intensity. In: *Neural Interfaces Conference*. 2016.
- Hubel DH, Wiesel TN.** Receptive fields, binocular interaction and functional architecture in the cat's visual cortex. *J Physiol* 160: 106–154, 1962.
- Jacobs AL, Fridman G, Douglas RM, Alam NM, Latham PE, Prusky GT, Nirenberg S.** Ruling out and ruling in neural codes. *P Natl Acad Sci Usa* 106: 5936–5941, 2009.
- Jenmalm P, Dahlstedt S, Johansson RS.** Visual and tactile information about object-curvature control fingertip forces and grasp kinematics in human dexterous manipulation. *J Neurophysiol* 84: 2984–2997, 2000.
- Jenmalm P, Johansson RS.** Visual and somatosensory information about object shape control manipulative fingertip forces. *J Neurosci* 17: 4486–4499, 1997.
- Johansson RS, Birznieks I.** First spikes in ensembles of human tactile afferents code complex spatial fingertip events. *Nat Neurosci* 7: 170–177, 2004.
- Johansson RS, Flanagan JR.** Coding and use of tactile signals from the fingertips in object manipulation tasks. *Nat Rev Neurosci* 10: 345–359, 2009.
- Johansson RS.** Tactile sensibility in the human hand: receptive field characteristics of mechanoreceptive units in the glabrous skin area. *J Physiol* 281: 101–125, 1978.
- Killebrew JH, Bensmaia SJ, Dammann JF, Denchev P V, Hsiao SS, Craig JC, Johnson KO.** A dense array stimulator to generate arbitrary spatio-temporal tactile stimuli. *J Neurosci Methods* 161: 62–74, 2007.
- Mackevicius EL, Best MD, Saal HP, Bensmaia SJ.** Millisecond Precision Spike Timing Shapes Tactile Perception. *J Neurosci* 32: 15309–15317, 2012.
- Mountcastle VB, Talbot WH, Darian-Smith I, Kornhuber HH.** Neural basis of the sense of flutter-vibration. *Science (80- )* 155: 597–600, 1967.
- Muniak MA, Ray S, Hsiao SS, Dammann JF, Bensmaia SJ.** The neural coding of stimulus intensity: linking the population response of mechanoreceptive afferents with psychophysical behavior. *J Neurosci* 27: 11687–11699, 2007.

**Pack CC, Bensmaia SJ.** Seeing and Feeling Motion: Canonical Computations in Vision and Touch. *PLoS Biol* 13: e1002271, 2015.

**Pawluk DT, Son JS, Wellman PS, Peine WJ, Howe RD.** A distributed pressure sensor for biomechanical measurements. *J Biomech Eng* 120: 302–5, 1998.

**Pawluk DT V, Howe RD.** A Holistic Model of Human Touch. *Comput Neurosci* : 759–764, 1997.

**Priebe NJ, Ferster D.** Mechanisms of Neuronal Computation in Mammalian Visual Cortex. *Neuron* 75: 194–208, 2012.

**Pruszynski JA, Johansson RS.** Edge-orientation processing in first-order tactile neurons. *Nat Neurosci* : 1–7, 2014.

**Saal HP, Bensmaia SJ.** Importance of spike timing in touch: an analogy with hearing? *Curr. Opin. Neurobiol.*, 2016.

**Scholl B, Tan AYY, Corey J, Priebe NJ.** Emergence of orientation selectivity in the Mammalian visual pathway. *J Neurosci* 33: 10616–24, 2013.

**Sripati AP, Yoshioka T, Denchev P V, Hsiao SS, Johnson KO.** Spatiotemporal receptive fields of peripheral afferents and cortical area 3b and 1 neurons in the primate somatosensory system. *J Neurosci* 26: 2101–2114, 2006.

**Talbot WH, Darian-Smith I, Kornhuber HH, Mountcastle VB.** The sense of flutter-vibration: comparison of the human capacity with response patterns of mechanoreceptive afferents from the monkey hand. *J Neurophysiol* 31: 301–34, 1968.

**Vallbo AB, Johansson RS.** Properties of cutaneous mechanoreceptors in the human hand related to touch sensation. *Hum Neurobiol* 3: 3–14, 1984.

**Victor JD, Purpura KP.** Metric-space analysis of spike trains: Theory, algorithms and application. *Network-Comp Neural* 8: 127–164, 1997.

**Weber AI, Saal HP, Lieber JD, Cheng J-W, Manfredi LR, Dammann JF, Bensmaia SJ.** Spatial and temporal codes mediate the tactile perception of natural textures. *Proc Natl Acad Sci* 110: 17107–17112, 2013.

**Witney AG, Wing A, Thonnard J-L, Smith AM.** The cutaneous contribution to adaptive precision grip. *Trends Neurosci* 27: 637–643, 2004.

## FIGURES

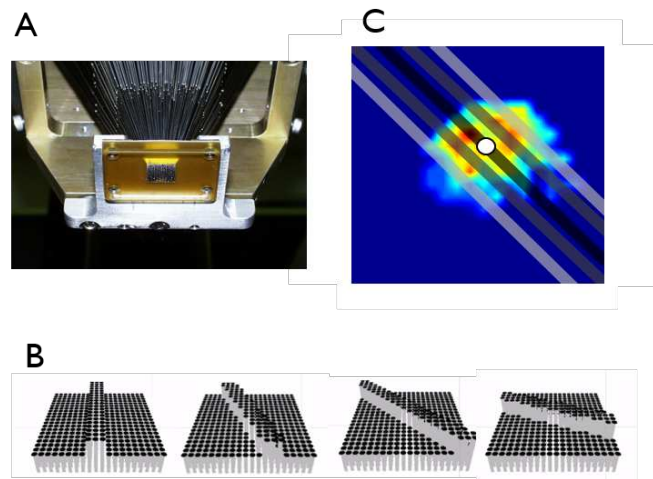


**Figure 1. Experimental set up.** A| Bottom view of the 400-probe stimulator (Killebrew et al. 2007). Individual pins converge onto a 1 cm<sup>2</sup> area over the skin. B| Sequence of snapshots depicting a bar indented at different edge orientations. C| Representation of a 135-degree bar indented at the hotspot and at two offsets from the hotspot. The heat map shows the RF topography. The overlaid black bar is centered on the hotspot, the dark and gray bars are displaced by  $\pm 1$  mm and  $\pm 2$  mm respectively. The hotspot is denoted by the white circle.

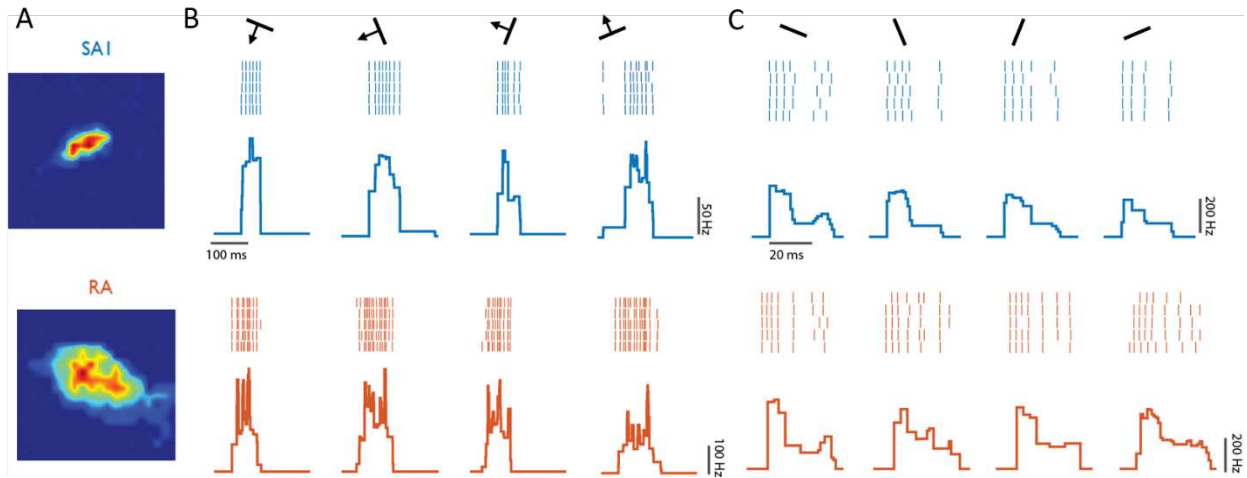


**Figure 2: Responses to oriented edges.** A | RF map for a typical SA1 (top) and RA (bottom) afferent. B | Rasters (for 5 repeats) and firing rate profiles to a bar scanned at a subset of orientations for the same two afferents (SA1 in blue, RA in orange). C | Responses evoked to indented bars at a subset of orientations for the same two afferents. Firing rate profiles are consistent within but vary across orientations for both scanned and indented bars.

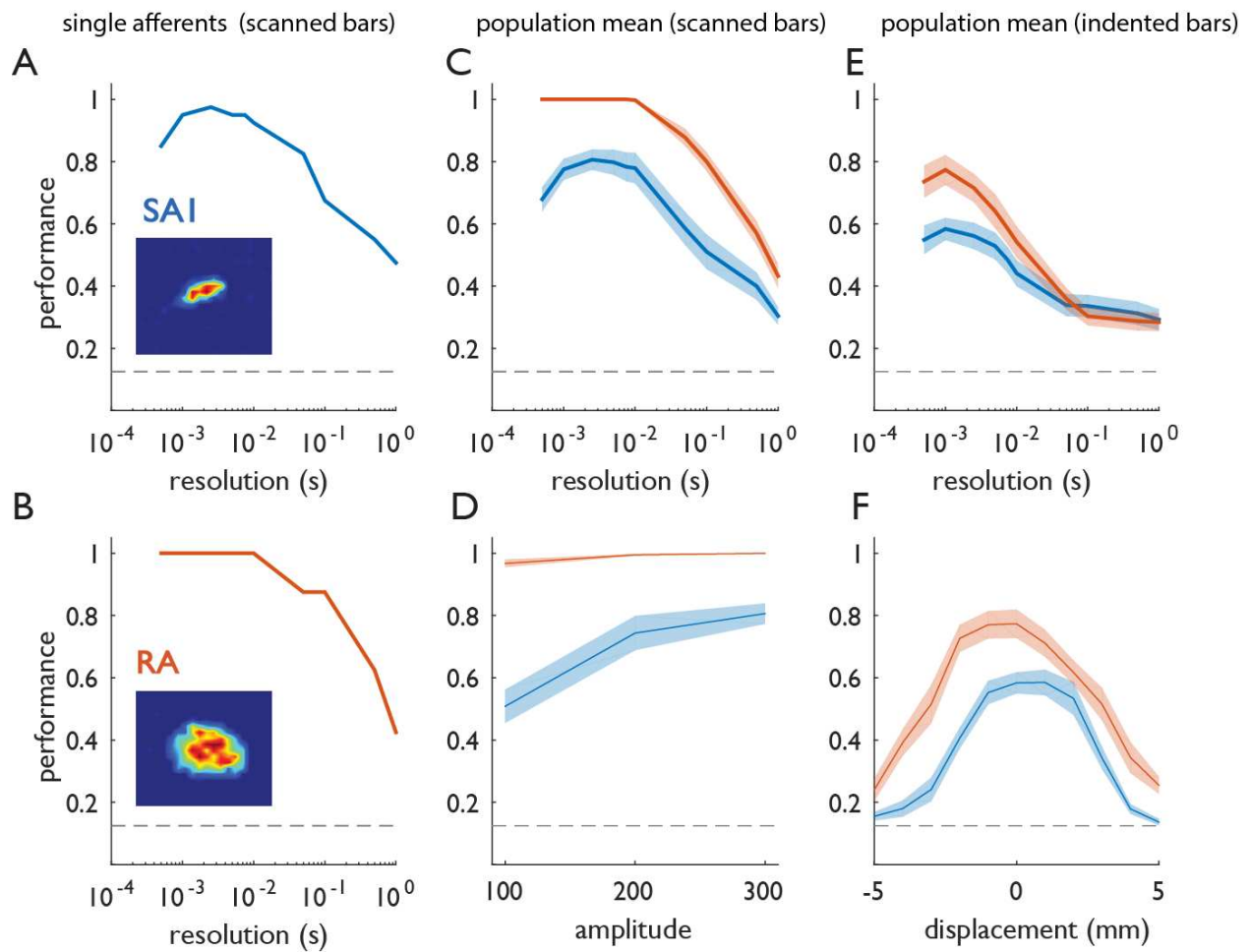


**Figure 3: Afferent orientation signals for scanned and indented bar stimuli.** A| Classification performance based on the responses of an SA1 afferent to 300- $\mu$ m scanned bars at 8 orientations as a function of the temporal resolution of the classifier ( $1/q$ ). The leftmost extreme of the curve shows classification performance when submillisecond differences in spike timing are taken into consideration, the rightmost extreme of the curve shows classification performance based solely on spike counts over the stimulus interval. B| Classification performance based on the responses of an RA afferent. C| Mean classification performance based on the responses of 10 SA1 (blue) and 12 RA fibers (orange) to scanned bars. D| Peak classification performance at three amplitudes. E| Mean classification performance based on the responses of 8 SA1 and 10 RA fibers to indented bars. F| Peak classification performance at different locations relative to the hotspot (located at displacement = 0 mm). In this analysis, classification is performed at each location separately. As was found in humans, tactile fibers carry considerable information about edge orientation in the precise timing of their responses. Error shading denotes standard error of the mean.

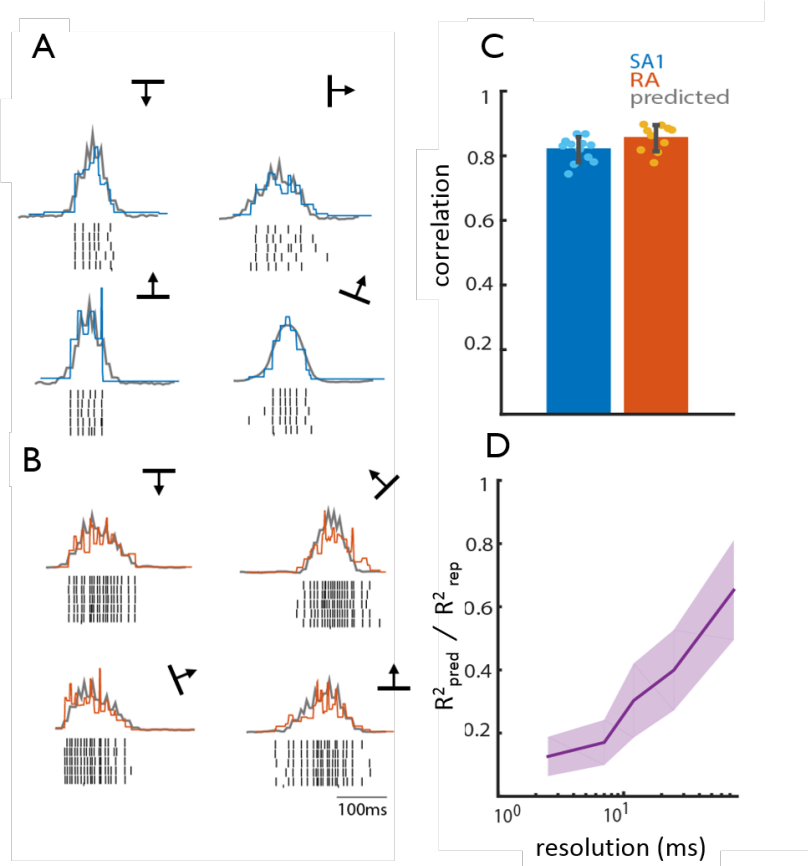


**Figure 1: Predicting the firing rate profiles from RF topography.** A| Example of predicted (gray) and observed (blue) firing rate profiles for a single SA1 afferent. B| Example of predicted (gray) and observed (orange) firing rate profiles for a single RA afferent. Although observed and predicted firing patterns are highly correlated, predicted firing patterns capture the coarse structure of the firing profiles, but not their fine structure. C| Mean maximum cross correlation between predicted and observed firing rate profiles for SA1 and RA afferent populations. The error bar represents the standard error of the mean. D| Ratio of  $R^2$  for predicted vs. observed ( $R^2_{pred}$ ) to the  $R^2$  for observed vs. observed ( $R^2_{rep}$ ) across multiple temporal resolutions. Error shading denotes standard deviation. Predicted firing rate profiles closely match observed firing rate profiles at coarse temporal resolutions, but not at fine ones.

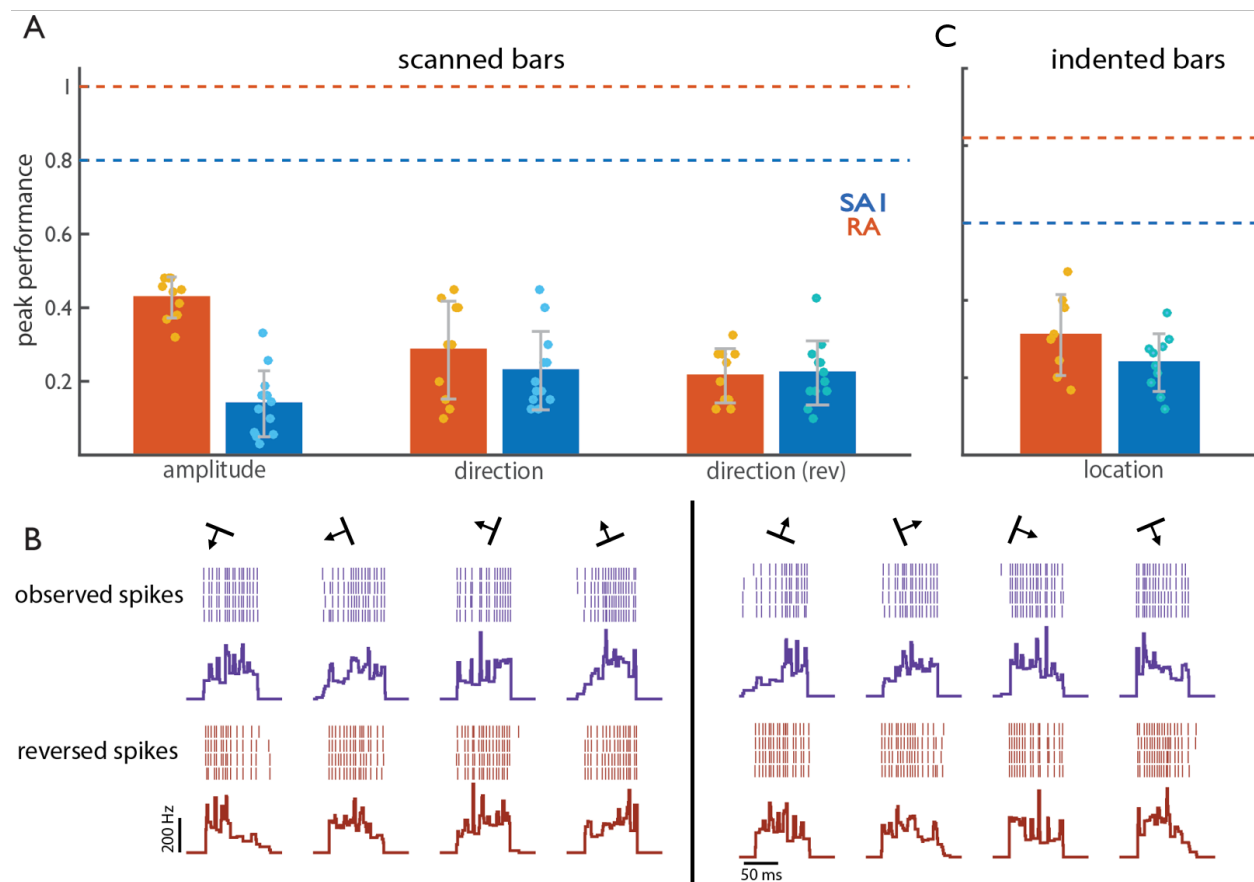


**Figure 5. Robustness of orientation signals.** A| Peak horizontal dashed lines denote peak classification performance when all other stimulus features are constant. Amplitude: Comparison of the responses at 100- $\mu$ m and 300- $\mu$ m to those at 200- $\mu$ m. Direction: Comparison of the responses in one direction to those in the opposite direction. Direction (rev): Comparison of the responses in one direction to reversed responses in the opposite direction. B| Example of spike patterns evoked from a single RA afferent for one scanned direction (left, purple rasters and mean firing rate profiles) and the opposite scanned direction (right, purple rasters and mean firing rate profiles). Reversed spike trains and mean firing rate profiles of the corresponding opposite scanned direction are displayed in red (bottom). C| Peak classification performance for indented bars at different locations. The horizontal dashed bars denote peak classification performance when the bar is centered on the hotspot, while chance levels are at 0.125. Grey bars represented standard error of the mean. Classification performance is substantially reduced when other stimulus features vary.